Optimization of University Campus Microgrid for Cost Reduction: A Case Study

Kayode Timothy Akindeji[1,2,a*], Remy Tiako[2,b] and Innocent Davidson[3,c]

[1,2]School of Electronic, Electrical and Computer Engineering, University of KwaZulu--Natal, Durban, South Africa

[3]Department of Electrical Power Engineering, Durban University of Technology, Durban 400, South Africa

[a]kayodea@dut.ac.za, [b]tiako@ukzn.ac.za, [c]innocentd@dut.ac.za

Abstract. This paper presents an optimization model to minimize the fuel cost and CO_2 emissions on university campuses using a hybrid renewable energy system (HRES). The HRES is made up of solar photovoltaic (PV), diesel generator (DG), wind turbine (WT) and battery energy storage system (BESS). Two university campuses are used as case studies to investigate the efficiency of the proposed HRES. The objective function is formulated such that each campus load is met by the renewable energy source (RES) when available and the DG only switches on when the output of the renewable energy source is not enough to meet the load. The resulting non-linear optimization problem is solved using a function in MATLAB called "quadprog". The results of the simulation are analyzed and compared with the base case in which the DG is used exclusively to meet the entire load. The results show the effectiveness of the optimized HRES in saving fuel when compared to the base case and reflect the effects of seasonal variations in fuel costs.

1. Introduction

The quality of life of people dwelling in rural or remote communities can be improved significantly through access to electricity. Geographical limitations and the high cost of grid extension are major difficulties responsible for the lack of electrification in these communities. Hence, off-grid microgrids are suitable solutions to overcome these challenges especially with the integration of renewable energy sources available free of charge within the communities. According to [1], a network system of distributed energy resources (wind turbine, solar PV, battery storage, and /or diesel generator) that is not connected to the grid is referred to as an autonomous or off-grid microgrid. Off-grid application of microgrid does not only help to reduce energy costs but also makes consumers energy independent. As reported in [2], the head office of Winkelmann Group based in Ahlen, Germany went off the European power grid in December 2018. The off-grid microgrid can produce 9 MW and 10 MW of electrical and thermal output respectively using six combined heat and power plants thereby reducing both electricity and grid usage costs. The off-grid application of microgrids is gaining more attraction for technical, environmental, and economical benefits.

Most off-grid applications of microgrid reported in the literature are for rural/remote area electrification [3-8], remote islands [9], military bases [10], and telecommunication base transceiver stations [11-13] while most university campus microgrids are grid-tied [14-17]. There are on going research towards achieving 100% renewable energy autonomy for university campuses. For instance, the authors of [18] investigated the integration of multiple renewable energy resources (solar PV, wind biomass) with or without energy storage with a view to attain reliable, safe, adequate and environmentally friendly energy system. This kind of hybrid energy system (HES) will replace the traditional power generating stations, reduce Greenhouse Gases (GHG) and preserve the earth for future generations. The authors proposed a PV/wind/biomass/pumped hyfro storage/battery hybrid system to meet the energy demand of the Middle East Technical University

(Northen Cyprus Campus). The results showed that the proposed HES gurantees 99% renewable energy fraction, that is almost 100% autonomy. Furthermore, Nesamaler et al. [19] carried out a study to investigate the technical and economic benefits of a HES at Kamaray College of Engineering and Technology (KCET), Tamu Nadu, India for both off-grid and on-grid modes. In addition, sensitivity analysis was carried out using solar radiation and fuel price as the sensitivity variables. The results indicated that the best system architecture for KCET is the on-grid HES using a load following dispatch strategy.

Another critical component of HRES is the control system which is carried out majorly through power electronic converters. The sources in the HRES must be controlled properly using certain power converter controllers to carry out power and voltage regulation in both grid-connected and standalone modes. In standalone mode, the source with stable output should be operated as a voltage controlled source to control the DC bus voltage while other sources operate as current control sources to manage power sharing among them [20]. According to Ammari et al. [21], control methods for HRES can be classified as centralize, distributed and hybrid. Distributed and hybrid methods are commonly used because of their efficiency, increased lifetime, low failure rate and the prospect of applying state-of-the-art control methods to individual component. In order to increase the efficiency and boost the operation of solar PV array, certain algorithm must be employed to control the operation of PV converters. In [22], the Perturb and Observe (P&O) maximum power point tracking (MPPT) algorithm was implemented. This algorithm is appropriate to be used for PV control systems due to its ease of implementation and simple structure. Also, it needs only two parameters as input, the PV voltage and current. Phan et al. [23] proposed a hybrid of P&O and Q Learning MPPT control algorirthm for a PV system. The results showed that a better performance when compared to the P&O method.

Considering the erratic load shedding experienced in South Africa in recent years, there is a need to consider the feasibility of the off-grid operation of university campuses for self-sustainability during load shedding. Lectures, practical experiments are disrupted and the entire university internet network (IP phones off) might be down because of load shedding. The objective of this study is to ensure continuous supply to critical loads using a hybrid system of diesel generator, solar PV, and battery storage. Therefore, the main goal of this work is to explore the feasibility of an off-grid HRES microgrid to meet the energy demand of a university campus at a minimum cost. The main contribution of this study is the investigation and optimal sizing of an off-grid hybrid system design proposed for two university campuses that comprises of PV, WT, DG, and battery considering two seasonal (winter and summer) and academic (study and vacation) periods.

2. Hybrid System Modelling and Configuration

The proposed hybrid power system in this study comprises solar PV, wind turbine, diesel generator, battery, and power converter as shown in Fig. 1. For power flow analysis, the control (communication) system has been omitted and is assumed to operate at an efficiency of 100%.

2.1 Solar Photovoltaic Model. The solar photovoltaic system consists of several solar photovoltaic cells connected in series to increase the voltage output and in parallel to increase the current. Numerically, the maximum power out of a PV module is the product of its maximum current and maximum voltage. However, the hourly energy output of the PV system can be described by Eqns. (1) to (3) [24, 25].
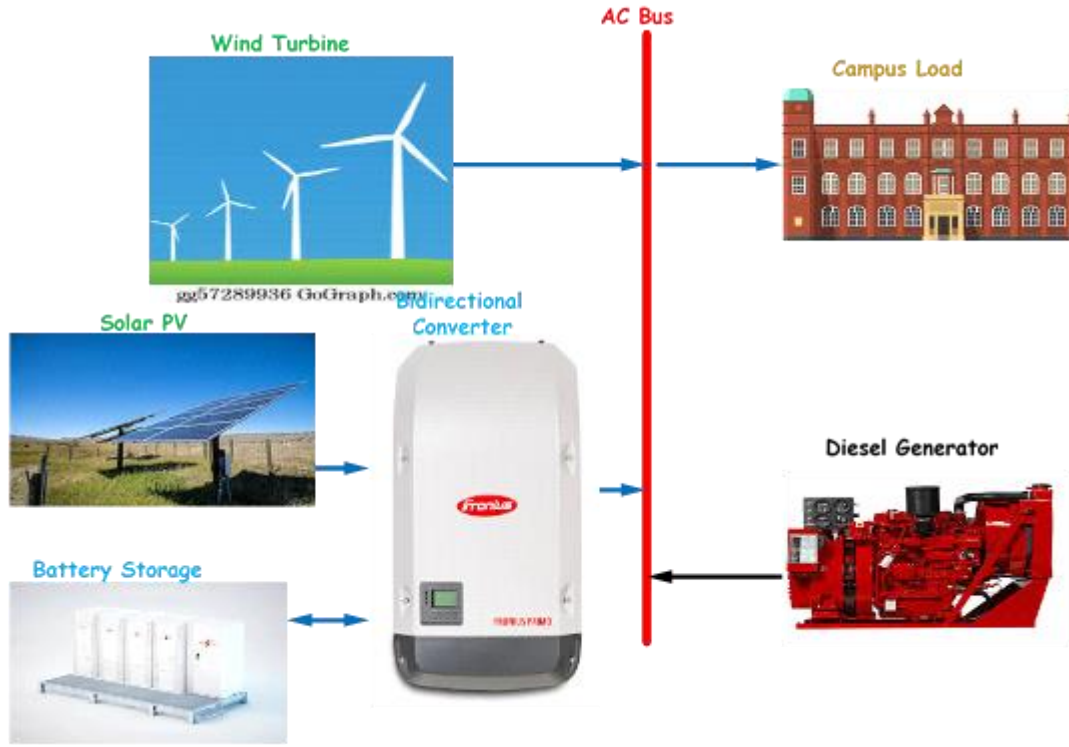
Fig. 1 Proposed Off-grid Hybrid Microgrid Configuration

$$E_{PV} = A_{ARR}.H_{Rad}\eta_{PV} \tag{1}$$

$$\eta_{PV} = \eta_{STC}(1 - \beta(T_C - T_{STC}))\eta_{INV} \tag{2}$$

$$T_C = T_a + \frac{SI}{SI_{NOCT}}(T_{NOCT} - T_{aNOCT}) \tag{3}$$

In equation (1), η_{PV} connotes the conversion efficiency (%) of the PV system, A_{ARR} is the PV array area (m^2), H_{Rad} is hourly solar irradiation (kWh/m^2) incident on the PV array. η_{STC} is the module efficiency at standard test condition (STC) (%), β is the temperature coefficient at the maximal power of the module (typically 0.004 – 0.005/°C), T_c is the PV cell temperature (°C), T_{STC} is the standard test condition temperature (25°C), η_{INV} is the inverter efficiency (%), T_a is the ambient temperature (°C), SI is the incident solar irradiance on the PV plane (W/m^2), SI_{NOCT} is the incident solar irradiance of 800W/m^2, T_{NOCT} is the nominal operating cell temperature (°C), and T_{aNOCT} is the ambient temperature for the nominal operating cell temperature (20°C). The output power of the PV array can also be determined using Eq.(4) [26],

$$P_{Arr} = N_P N_S P_{max}\eta_{MPPT} L \tag{4}$$

Where P_{max} represents the maximum power of the PV module, N_P and N_S are the numbers of parallel and series-connected modules respectively. η_{MPPT} is the MPPT efficiency and L is loss in the system.

2.2. Wind Turbine. Wind turbines are categorized into two designs according to their orientation of the axis of rotation. Horizontal axis wind turbine (HAWT) has its axis of rotation parallel or horizontal with the ground while vertical axis wind turbine (VAWT) axis of rotation is perpendicular or vertical to the ground. The HAWT is preferred for electrical power generation due to its higher conversion efficiency and access to stronger wind at higher hub height [26, 27]. The

major components of a HAWT and its configuration are shown in Fig. 2. Therefore, this work considered a HAWT with three blades. The power output of a WT is a function of certain parameters such as air density, wind speed at the particular location, area swept by rotor blade and energy conversion efficiency. The mechanical power output, P_{mech}, of a WT is given by:

$$P_{mech} = 0.5C_{cp}\rho AV^3 \tag{5}$$

Where C_{cp} is the power coefficient and is a function of the tip-speed ratio and the blade's angle. V is the wind speed (m/s), A is the area swept by the blade (m^2) and ρ is the air density (kg/m^2). It should be noted however that the effective wind speed is usually at 50-100m above ground level. Hence, the wind speed measured by the anemometer at a reference height must be converted to a new value at the actual hub height using Eq. 6 [26, 28].
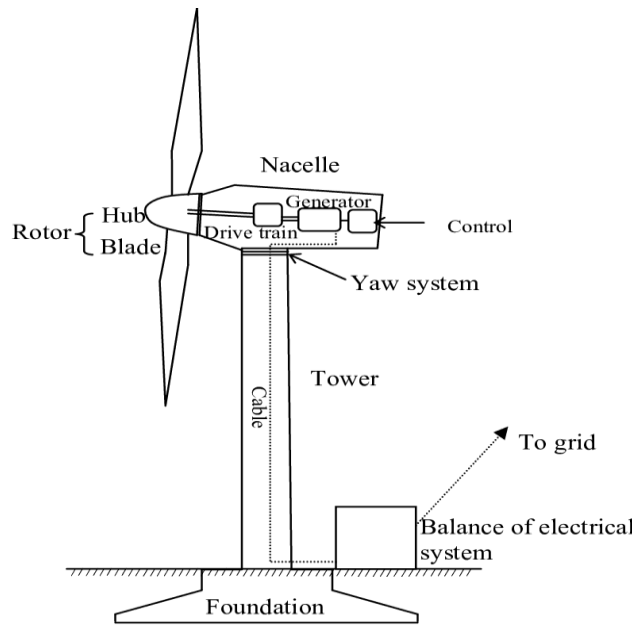

Fig. 2 Components of HAWT [29]

$$V_{new} = V_{ref}\left(\frac{h_{new}}{h_{ref}}\right)^{\alpha} \tag{6}$$

Where V_{new} and V_{ref} are the wind speeds at the desired hub height h_{new} and the reference height h_{ref} respectively and α is the power-law exponent, representing the friction coefficient of the ground surface. V_{new} is used in modeling the power output to calculate the power produced by the wind turbine. Eq. 7 gives an approximation of power generated from the wind turbine depending on the performance curve of the wind turbine.

$$P_w = \begin{cases} 0 & ;V \leq V_{in} \geq V_{out} \\ V^3\left(\dfrac{P_{rated}}{V_{rated}^3 - V_{in}^3}\right) - P_{rated}\left(\dfrac{V_{in}^3}{V_{rated}^3 - V_{in}^3}\right) & ;V_{in} \leq V \leq V_{rated} \\ P_{rated} & ;V_{rated} \leq V \leq V_{out} \end{cases} \tag{7}$$

Where P_W represents the power produced by the wind turbine, V is the wind speed, V_{in} and V_{out} are the cut-in wind speed and the cut-out wind speed of the wind turbine respectively. P_{rated} and V_{rated} are respectively the rated power and rated speed of the wind turbine. This work adopted a mathematical model proposed in [26]to determine the electrical power from the hourly wind speed as given by Eq.8.

$$P_{elect} = 0.5\eta_{wt}C_{cp}\rho AV^3 \tag{8}$$

Where η_{wt} represents the efficiency of the wind turbine as stated in the manufacturer's datasheet.

2.3. Diesel Generator. Without the connection to the local electricity grid, reliability of supply is crucial for the operation of off-grid microgrid. DGs are included in hybrid systems to act as backup during the period when the renewable energy sources cannot meet the load demand, thereby ensuring system reliability. To deploy DG in hybrid system, it is important to consider the operating limits of the DG as recommended by the manufacturer. Therefore, the operation of the DG at any instance must be within the rated power and stated minimum value (because maximum efficiency of the DG correlates with its rated power) this constraint is expressed in Eq.9.

$$P_{dg}^{min} \le P_{dg}(t) \le P_{dg}^{max} \tag{9}$$

The rate of fuel consumption (directly proportional to fuel cost) is modelled using Eq.10

$$FC(t) = \alpha P_{dg}(t) + \beta P_{dg,rated}(t) \tag{10}$$

FC(t) is the fuel consumption rate(l/h), $P_{dg}(t)$ represents the power output of DG and $P_{dg,rated}$ is the DG rated capacity (kW). α and β are the fuel curve intercept coefficient (l/h/kW) and the diesel curve intercept coefficient (l/h/kW) respectively. For the economic operation of the hybrid system, a load-following dispatch strategy is used whereby the DG is turned on when the renewable energy source and/or the battery cannot supply the load.

2.4. Battery Storage. Battery energy storage systems are included in the hybrid system due to the following:

- Stochastic and intermittent nature of renewable energy source
- Reduction of fuel cost and CO_2 emission
- Maintenance of system stability i.e. balance between load and supply
- Storage of excess energy produced by renewable energy source

The battery system (battery bank) in this work is designed to be charged during excessive production of renewable energy source and discharged when the renewable energy source output cannot meet the load demand. For off-grid application, the battery must be operated within the minimum and maximum limits of their state of charge (SoC) as stated by the manufacturer. SoC of a battery simply expresses the battery charge level relative to its capacity at a specific time (hour). The SoC of the battery at any time (hour) is given by Eq.11.

$$B_{soc}(t) = B_{soc}(t-1) + \eta_c P_{bc}(t) - \eta_d P_{bd}(t) \tag{11}$$

Where η_c and η_d are the battery charging and discharging efficiencies respectively. P_{bc} and P_{bd} are the power received and emitted by the battery at the time, *t* respectively. Considering the battery dynamics, Eq.11 can be simplified further as:

$$B_{soc}(t) = B_{soc}(0) + \eta_c \sum_{t=1}^{N} P_{bc}(t) - \eta_d \sum_{t=1}^{N} P_{bd}(t) \tag{12}$$

Where $B_{soc}(0)$ is the initial battery SoC.

To increase the life span of the battery, the battery operation must be governed by these constraints:

$$B_{cap}^{min} \le B_{cap}(t) \le B_{cap}^{max} \qquad \text{and} \qquad B_{cap}^{min} = (1 - DoD)B_{cap}^{max} \tag{13}$$

Where DoD is the depth of discharge in percentage.

2.5. Converter and Control System. In order to draw out maximum power from the renewable energy sources, suitable power electronics converters and appropriate control strategies must be employed. The control of HRES is essential to improve the productivity and reliability of a power system that operates under the unpredictability of renewable energy resources and active loads [22, 23]. Parameters to be controlled in a HRES include:

- Frequency and voltage for stability

- Power flow for protection

- Power balance between source and load.

Maximum power point tracking (MPPT) based on different optimization algorithm are applied to both wind turbine and solar PV for optimal performance. The control of DG focuses more on frequency control voltage control and reactive power [21]. Hence, in this work, the DG is modelled as a controllable variable power source with minimum and maximum output power. The battery control is such that no power flow more than the maximum permissive power is allowed. Energy management of the HRES is ensured by making the total power generated from the renewable energy source (PV and wind turbine) the main power supply that must be used to meet the load demand first before the other sources (Battery and DG).

3. Optimization Model

The hybrid power system is designed such that, priority is given to the renewable energy source (PV and WT) in meeting the load, when and if the renewable energy source output is not adequate to supply the load, the battery discharges provided that it is within its operating limits. The diesel generator is switched on only if the renewable energy source and battery are unable to meet the power demand, meaning that the diesel generator is kept at the least demand. In the case whereby the maximum demand is met only by renewable energy source, thereafter the surplus energy generated by the renewable energy source is stored in the battery. Fig. 3 shows the flow chart that illustrates the simulation and optimization process while the parameters of the simulation model are provided in Table 1.

3.1. Formulation of Objective Function. The hybrid system is optimized to minimize the power supplied by the DG. This is achieved by formulating the optimization problem to minimize the cost of fuel consumed by the DG during the operating time. The fuel cost, F_{cost} of the DG is a quadratic non-linear function as in Eq.14

$$F_{\cos t} = C_f \sum_{k=1}^{N} (aP_{dg(k)}^2 + bP_{dg(k)} + c) \tag{14}$$

Where a, b, and c are the generator cost coefficient (available in the manufacturer's datasheet), C_f is price per litre of diesel fuel, N represents the number of DG. Therefore, the objective function is expressed as:

$$\min F_{\cos t} = C_f \sum_{k=1}^{N} (aP_{dg(k)}^2 + bP_{dg(k)} + c) \tag{15}$$

Subject to the following constraints:

$$P_{pv}(k) + P_{wt}(k) + P_{bd}(k) - P_{bc}(k) + P_{dg}(k) = P_d(k) \tag{16}$$

$$P_{pv}(k) \geq 0, P_{wt}(k) \geq 0, P_{bc}(k) \geq 0, P_{bd}(k) = 0, P_{dg}(k) \geq 0 \tag{17}$$

$$B_{soc}^{\min} \le B_{soc}(0) + \eta_c \sum_{k=1}^{N} P_{bc}(k) - \eta_d \sum_{k=1}^{N} P_{bd}(k) \le B_{soc}^{\max} \tag{18}$$
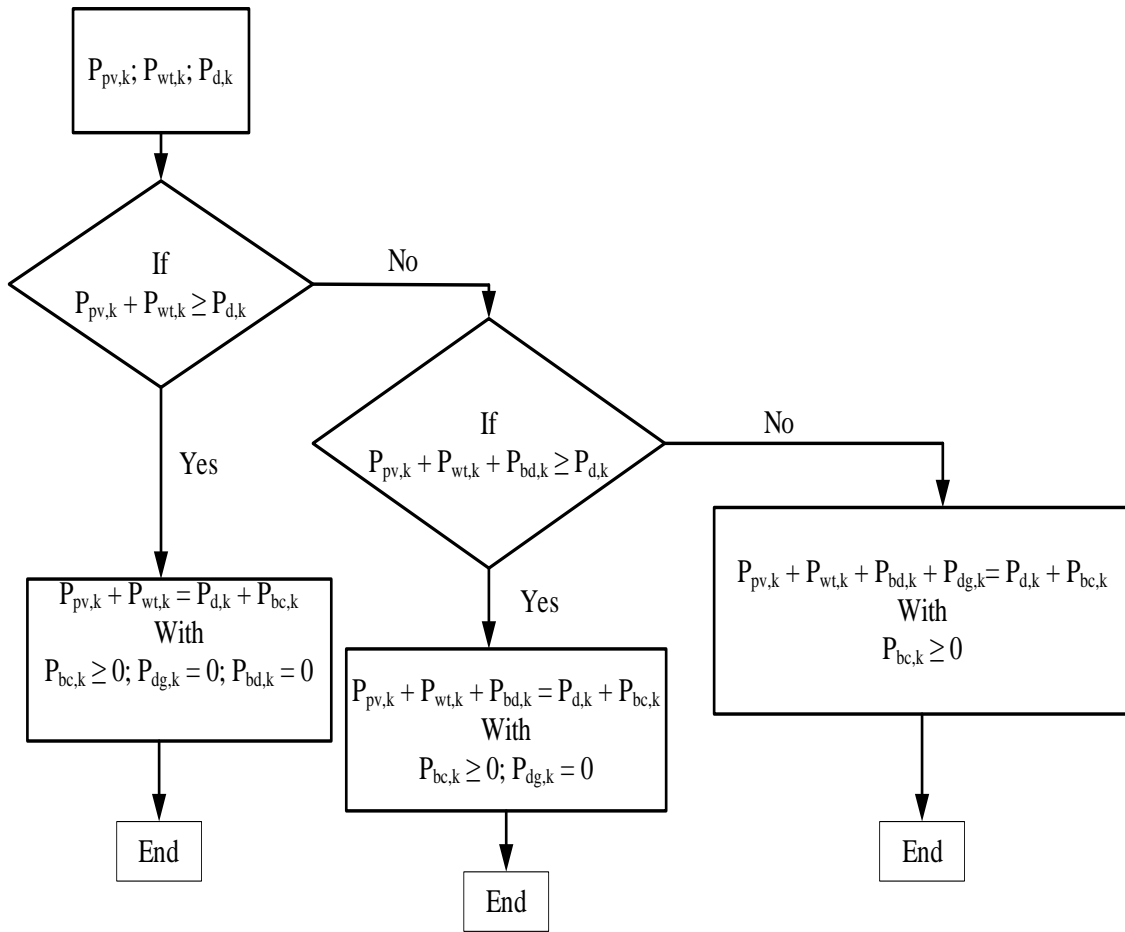
Fig. 3 Flow chart for the optimization process

For all k = 1,...., N, where N is 24 i.e number of hours in a day. $P_{pv(k)}$, $P_{wt(k)}$, $P_{bd(k)}$, and $P_{dg(k)}$ represent variables of energy flowing from the solar PV, wind turbine, battery and diesel generator respectively to the load at any time (k) while $P_{bc(k)}$ is the energy flow to the battery.

The non-linear optimization is solved by using a function in MATLAB, called "quadprog". This function finds the minimum for problems in the form:

$$\min \frac{1}{2} x^T H x + f^T x \text{ such that } \begin{cases} A.x \le b, \\ Aeq.x = beq, \\ lb \le x \le ub. \end{cases} \tag{19}$$

A, H and, *Aeq* are matrices, and *b, f, beq, lb, ub,* and x are vectors.

3.2. Load Model. Four load models of two campuses (Howard and PMB) are considered for this study; these are daily load profiles for typical days during summer and winter based on the 2019 university sessional calendar.

Table 1 Simulation parameters

Solar PV	
Parameters	Values
PV array area	1000m^2
Geometric factor	0.6
incident solar irradiance at nominal operating cell temperature	0.8 kWh/m^2
Cell temperature	45°C
Ambient temperature for the nominal operating cell temperature	20°C
Standard test condition temperature	25°C
PV generator efficiency measured at reference cell temperature	0.17
β, temperature coefficient at the maximal power of the module	0.004/°C
Wind Turbine	
Parameters	Values
Hub height	80m
Reference height	42m
Blade diameter	1.5m
Turbine efficiency	95%
Cut out speed	20m/s
Cut in speed	3m/s
Rated speed	10m/s
Rated power	500kW
Friction coefficient	0.25
Number of units	10
Turbine efficiency	95%
Diesel Generator	
Parameters	Values
Fuel cost	$1.2/litre
Capacity	200kVA
Number of units	18
Battery	
Parameters	Values
Battery charge efficiency	85%
Battery discharge efficiency	100%
Maximum capacity	500kWh

4. Simulation Results and Discussion

This section discusses the simulation results of the hybrid power system simulated under different load and meteorological conditions. The costs of using only the DG to supply the load are also compared to the costs of using the hybrid system.

4.1. Howard College Campus. Table 2 presents the load data for the Howard campus, these are daily load data for selected days during summer study period (4 February – 31 May 2019), summer vacation (13- 22 April 2019), winter study period (8 July -31 August 2019) and winter vacation (14 June – 7 July 2019). Fig. 4 shows the four load profiles together (to illustrate the variations), it is observed that the demands begin to rise from 07h00, peak between 11h00 and 13h00 and start decreasing from 16h00 to 19h00 (closing hours), a small rise is observed between 21h30 and 22h30. The load demands for the selected days are met by a combination of energies supplied by the DG, solar PV, wind turbine and battery. It is observed that the two demands during summer are higher than the two demands during winter. This is however contrary to what is expected as the utility regards the winter period as high demand period hence higher tariff. The obvious reason is the use of air conditioners in most offices and lecture rooms during the summer; moreover, it is easier for

staff members and students to dress warmly during winter. In addition, the city of Durban has temperate weather during winter compared to other cities in South Africa.

i. ***Summer Study day.*** Before sunrise, that is between 00h00 and 08h00, the load was met by the DG and battery, the PV started generating from 08h00 while the WT started at 12h00. As observed in Fig. 5, as the wind speed increased and the PV continued to produce energy, the load was met majorly by the WT and PV between 12h00 and 20h00. For instance, at 15h00, the load demand was 3622 kW, this was supplied by the WT (3335.09 kW) and PV (286.91 kW). The DG switched off (15h00 – 20h00) the moment the renewable energy source output was enough to meet the load and the battery were charged during this period. The setup ensures that the operating time and output of the DG depend on the power produced by the renewable energy source (PV and WT). Therefore, the more the output of the renewable energy source, the less the DG output hence lower operating (fuel) cost. The PV started generating earlier than the WT, however, the WT continued to generate after the sunset. With this pattern, the renewable energy source was able to compliment the energy supply for about 15 hours of the day.

Table 2 Demand Profiles for Howard Campus

| Time	Summer Load (kW)		Winter Load (kW)	
	Study	Vacation	Study	Vacation
00:30	2,612.06	1,670.39	1,758.59	1,636.91
01:30	2,310.82	1,613.54	1,702.42	1,574.54
02:30	2,249.62	1,579.61	1,595.80	1,567.30
03:30	1,967.64	1,549.60	1,584.86	1,589.80
04:30	1,971.71	1,542.62	1,576.28	1,590.22
05:30	2,096.10	1,625.54	1,633.67	1,684.50
06:30	2,005.98	1,924.85	1,870.40	1,728.78
07:30	2,491.91	2,043.71	2,328.35	1,739.16
08:30	3,216.86	2,652.66	2,700.31	1,957.18
09:30	3,593.82	2,836.68	2,929.39	2,049.89
10:30	3,720.29	2,935.10	3,015.71	2,137.07
11:30	3,739.58	2,964.55	2,993.03	2,084.26
12:30	3,721.79	2,988.95	3,071.75	2,114.97
13:30	3,724.31	2,861.23	3,052.78	2,138.02
14:30	3,622.14	2,883.00	3,037.42	2,110.50
15:30	3,322.96	2,757.83	2,898.32	2,112.95
16:30	3,034.11	2,659.24	2,661.63	1,954.27
17:30	2,726.58	2,430.02	2,359.38	1,745.69
18:30	2,119.60	2,045.60	2,397.89	1,677.28
19:30	2,176.31	1,901.37	2,364.23	1,654.56
20:30	2,102.51	1,916.17	2,197.84	1,573.03
21:30	2,428.05	2,072.12	2,332.27	1,981.02
22:30	2,464.73	2,170.98	2,232.38	1,779.10
23:30	2,231.77	1,712.30	2,041.67	1,661.08
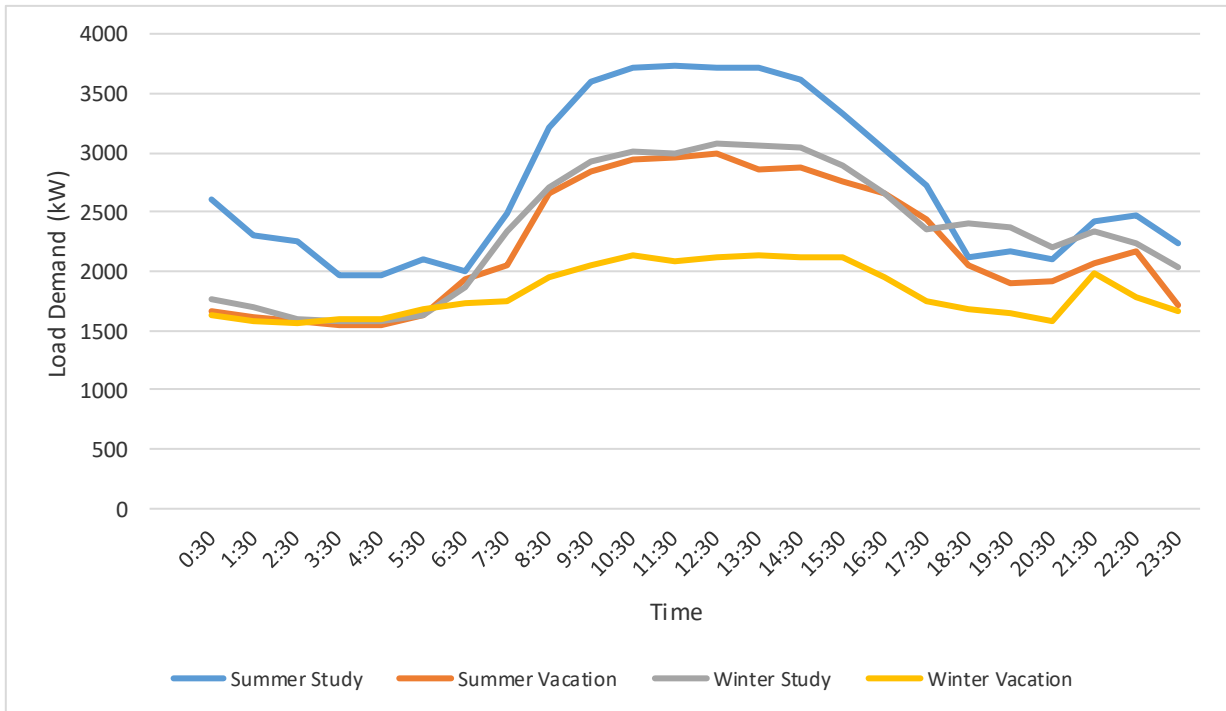
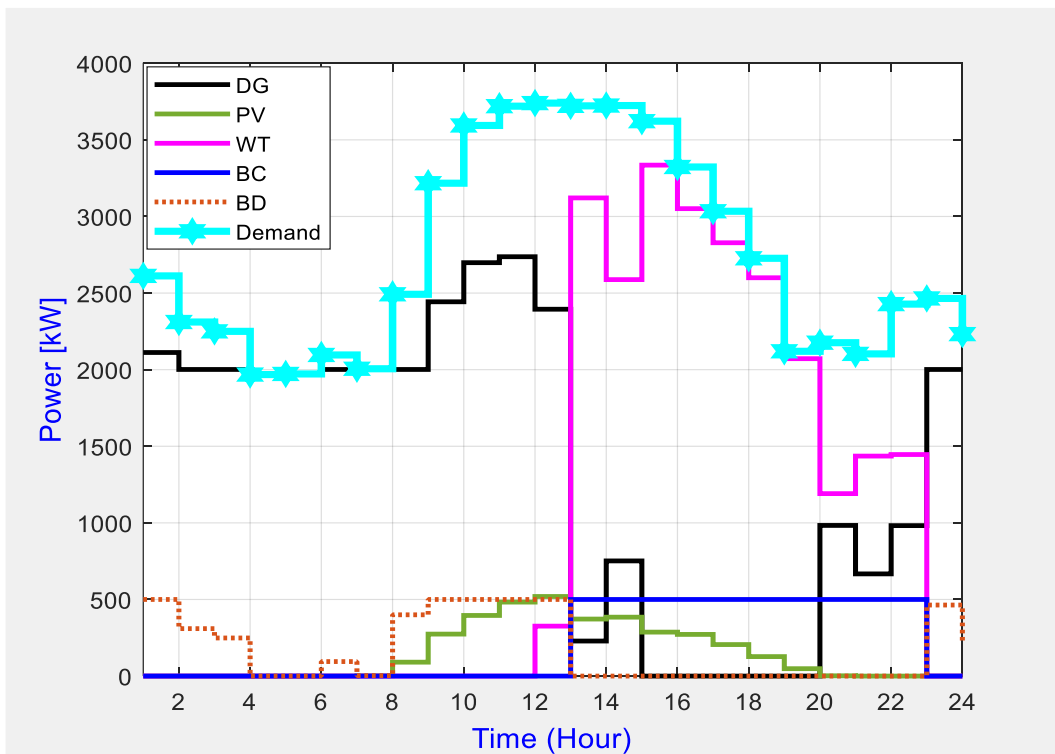Fig. 4 Howard campus load profiles

Fig. 5 Summer Study day (13 March 2019) Power Flow

ii.　***Summer Vacation day.*** The energy flow for this day is shown in Fig. 6, the load profile for the day shows a decline in the load demand throughout the 24 hours compared to a typical study day confirming fewer academic activities on campus. The wind speed throughout the day was below the cut-in speed (3.5 m/s), the maximum speed on the day was 2.157 m/s, and hence there was no generation from the WT. The load was supplied by the DG only in the early hours of the day until the sun rose at 09h00. As the PV started generating, the output of the DG reduced gradually until the sun went down and the DG supplied the load for the remaining hours of the day. The peak load (2989 kW) on the day occurred at 13h00 and was

supplied by the DG (2317.41 kW) and PV (671.59 kW). As observed, the PV was able to supply part of the peak load period hence served as peak shaving.
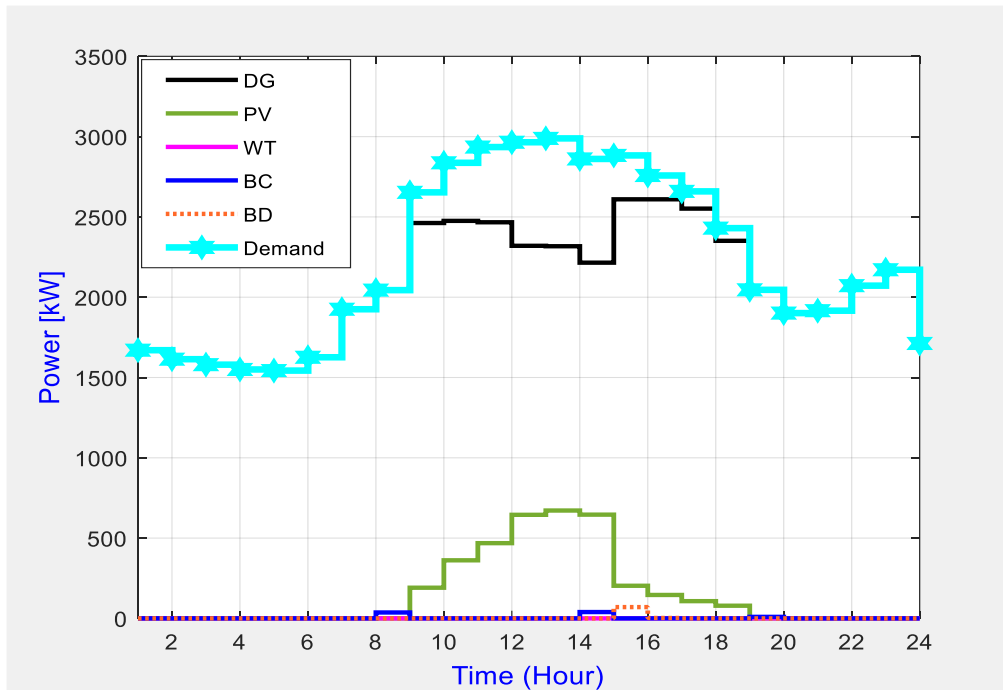

Fig. 6 Summer Vacation day (17 April 2019) Power Flow

iii.   **Winter Study day.** The generation-demand profile for this scenario is shown in Fig. 7. It is generally observed that the DG supplies the bulk of the power required to meet the load throughout this period. Likewise, the demand is lowest in the first-third (00h00 to 08h00) of the day, highest in the second-third, and median in the final third of the day. It is also observed that the PV generation begins to ramp up at 09h00 till 15h00, reducing the DG generation within this period, and the PV generation declines gradually after 15h00. The WT has a zero generation for most of this scenario, however, a short-spanned generation between 16h00 to 18h00 and 19h00 to 20h00. It can be concluded that fuel cost as a result of the bulk DG generation in this scenario would be higher than the summer study period that experienced higher PV and WT generation to offset the demand.

iv.   **Winter Vacation day.** The winter vacation day scenario is a peculiar scenario that experiences the least renewable energy generation and net demand when compared to the previous scenarios. From Fig. 8, it is observed for most of the day, the DG supplies all the demand with near-zero generation from the WT. The PV generation in this scenario has a gaussian distribution with peak generation between 13h00 to 15h00. Similar to the winter study day, this scenario has a higher fuel cost and CO_2 emissions when compared to the summer vacation day.

The summary of the fuel cost of these scenarios comparing the 'DG only' and 'hybrid' modes is represented in Table 3. It can be inferred that the summer study day has the highest fuel cost in the DG only mode, however, in the hybrid generation mode, the summer vacation day has the highest fuel cost. Therefore, it can be concluded that the summer period incurs more fuel costs than the winter period at the Howard campus. However, the summer study period has the least fuel cost in the hybrid mode, indicating the highest penetration of PV, WT, and Battery sources. Consequently, the fuel-saving cost is highest in the summer study period. It can be observed that the generation in both modes for the summer vacation and the two winter scenarios are marginally different due to the low generation from the renewable energy sources, thus, the fuel savings are marginal in these scenarios.
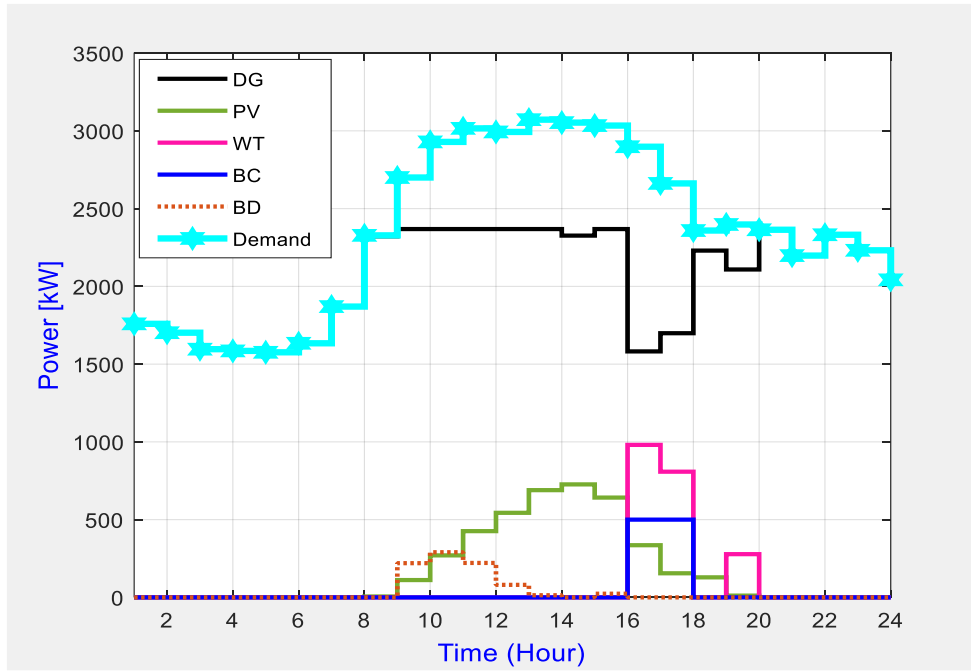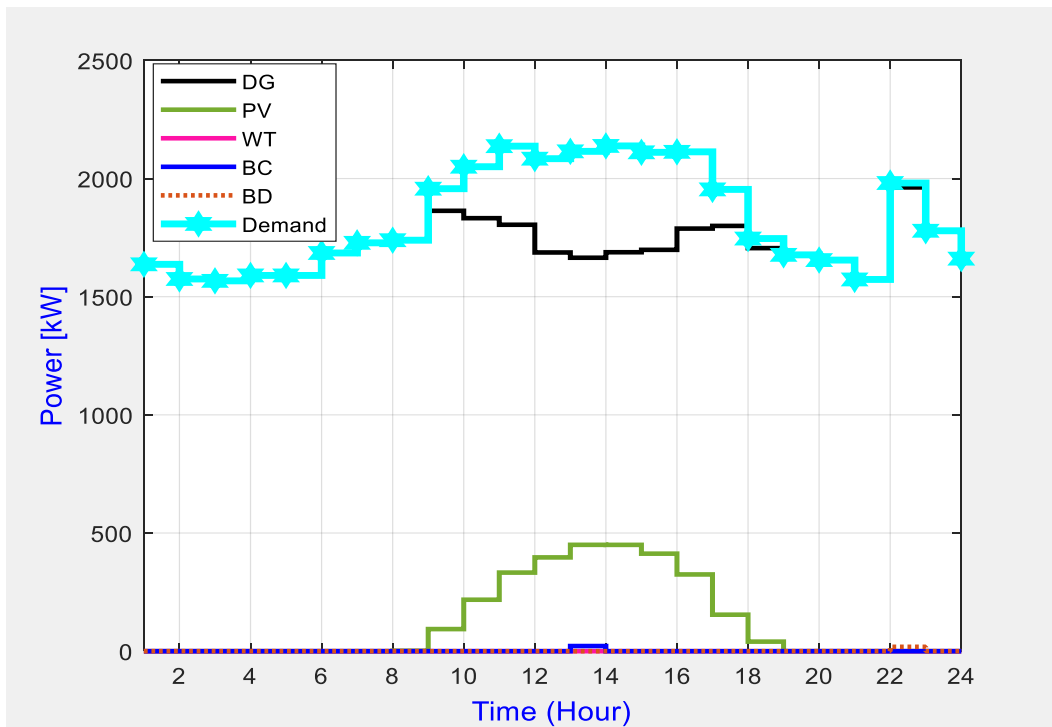
Fig. 7 Winter Study day (13 August 2019) Power Flow

Fig. 8 Winter vacation day (25 June 2019) Power Flow

Table 3 Fuel Cost Saving

	Summer ($/h)		Winter ($/h)	
	Study	Vacation	Study	Vacation
DG Only	65.65	53.34	56.33	43.84
Hybrid	33.95	49.75	49.37	40.95
Saving	**31.70**	**3.59**	**6.96**	**2.89**

4.2. Pietermaritzburg Campus.

i.   Summer study day. The generation-demand pattern for this scenario is depicted in Fig. 9, it is seen that at the start of the day (00h00 to 08h00), all of the demands are met by the DG with a transient WT generation between 02h00 to 03h00. As the day begins to brighten, the PV starts to generate electricity, reducing the power supply from the diesel generator.

Table 4 Demand Profiles for PMB Campus

Time	Summer (kW)		Winter (kW)	
	Study	Vacation	Study	Vacation
00:30	1,718.00	1,586.00	1,847.00	1,492.00
01:30	1,630.00	1,445.00	1,811.00	1,512.00
02:30	1,582.00	1,354.00	1,674.00	1,487.00
03:30	1,530.00	1,318.00	1,596.00	1,460.00
04:30	1,433.00	1,265.00	1,651.00	1,443.00
05:30	1,407.00	1,277.00	1,647.00	1,436.00
06:30	1,539.00	1,386.00	1,724.00	1,559.00
07:30	1,756.00	1,526.00	1,783.00	1,881.00
08:30	1,986.00	1,645.00	1,878.00	1,987.00
09:30	2,311.00	1,811.00	1,956.00	2,095.00
10:30	2,542.00	2,003.00	1,958.00	2,205.00
11:30	2,641.00	1,971.00	2,024.00	2,174.00
12:30	2,649.00	2,074.00	2,029.00	2,128.00
13:30	2,684.00	1,936.00	2,001.00	2,045.00
14:30	2,657.00	2,004.00	2,054.00	2,082.00
15:30	2,711.00	2,043.00	2,021.00	2,019.00
16:30	2,609.00	2,049.00	1,986.00	2,006.00
17:30	2,339.00	2,001.00	1,976.00	1,831.00
18:30	2,123.00	1,945.00	2,061.00	1,825.00
19:30	2,216.00	1,940.00	2,136.00	1,784.00
20:30	2,245.00	1,909.00	2,094.00	1,793.00
21:30	2,104.00	1,802.00	2,118.00	1,743.00
22:30	2,017.00	1,627.00	2,030.00	1,655.00
23:30	1,877.00	1,584.00	1,913.00	1,595.00

The excess generation in this period is stored in the battery. During the peak demand (10h00 to 18h00) when several activities are ongoing at the campus, the PV and DG supply the load with relatively low support from the WT. Towards the end of the day when the sun sets, the DG meets the demand operating maximum capacity, however, the total demand is greater than the DG power output. Thus, the battery discharges power to offset the power shortage that may lead to frequency instability or load shedding on campus.
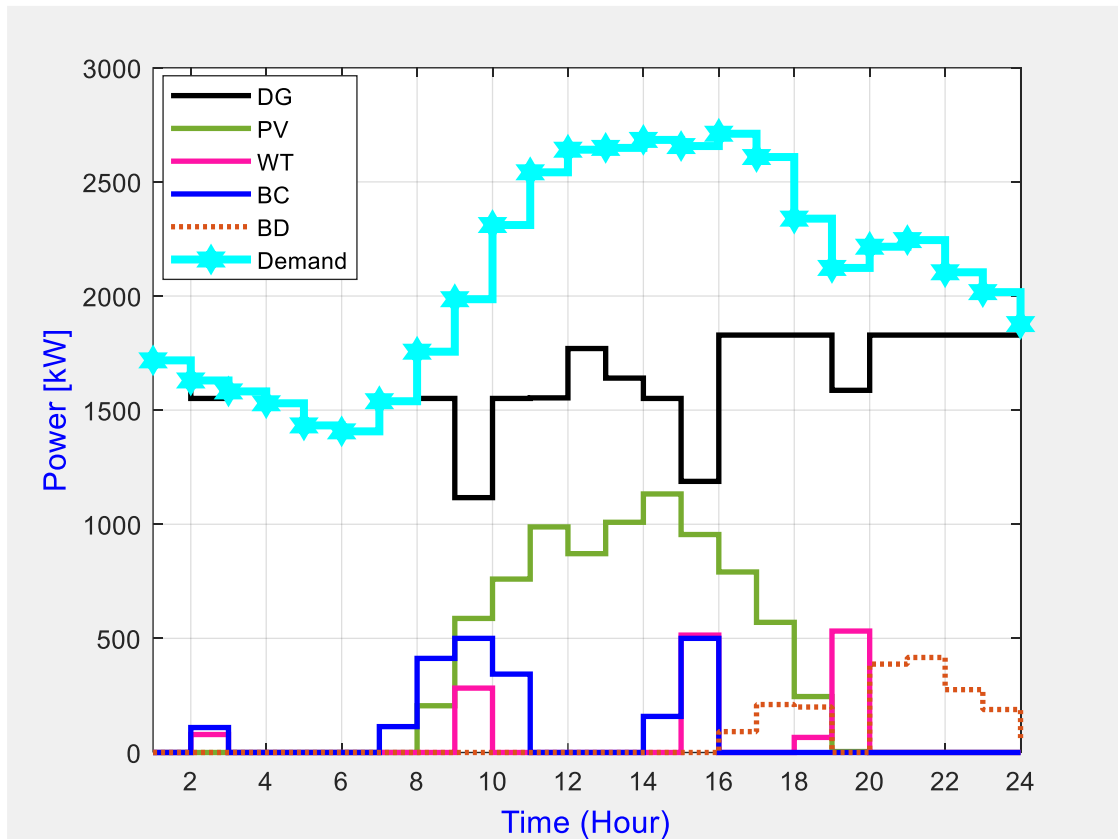
Fig. 9: Summer Study day (13 March 2019) Power Flow

ii. Summer vacation day. In contrast to the summer study day, the summer vacation day experienced a high penetration of WT generation in the energy mix with peak generation between 15h00 to 21h00 as depicted in Fig. 10. To this effect, a high share of the demand is supplied by the WT with support from the DG when needed. The cumulative time for excess generation is 10 hours, part of which is stored in the battery. It is observed that there is intermittence in the PV and WT outputs, while the DG is already operating at full capacity to meet the load, the battery supports during this scenario by dissipating power to balance the total generation and total demand. Another inference is the shut down of the DG for 7 hours when there is sufficient renewable energy penetration thereby saving fuel cost and reducing CO_2 emissions.

iii. Winter Study Day. This day experiences a high share of WT generation, similar to the summer vacation day. As expected, the PV generation is low due to low irradiance in the winter season. Fig. 11 shows the generation-demand pattern for a typical study period during the winter season at the Pietermaritzburg campus. The demand profile has an approximate uniform distribution with some deviation in the first third of the day. The bulk of the demand is met by the DG and WT, with the DG meeting the demand in the morning and the WT generating power in the afternoon period. The excess power generated during the day is stored in the battery, and dissipated at night (00h00 to 04h00 and 19h00 to 24h00) to support the DG output.

iv. Winter Vacation Day. The winter vacation day on the Pietermaritzburg campus has a generation-demand profile shown in Fig. 12. It is observed that is high WT generation on this day such that the DG is active for only 4 hours. Similarly, the excess generation is continually stored in the battery. The PV generation on this day is low due to the low irradiance in the winter season. In contrast to other scenarios where the DG is always active in the early hours of the day, it is observed that on the winter vacation day, the WT generates sufficient power needed to meet the load during this period and the support from the PV in the midday period is enough to balance the generation.
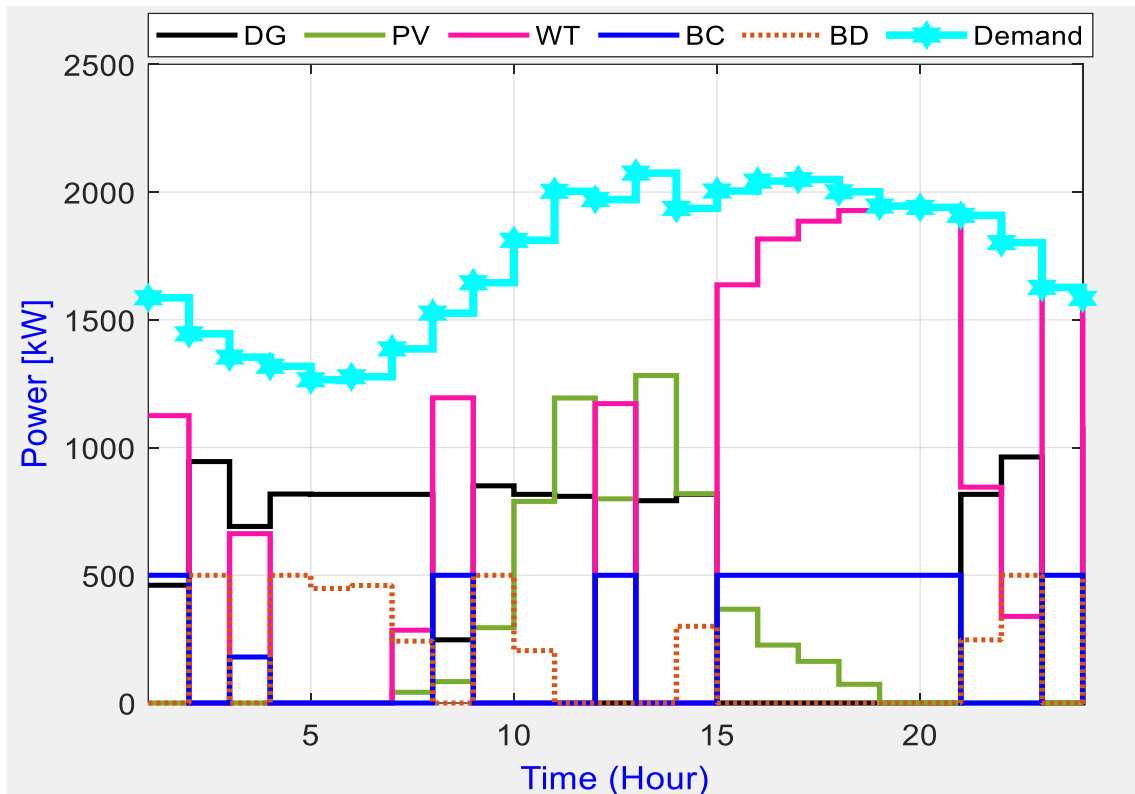
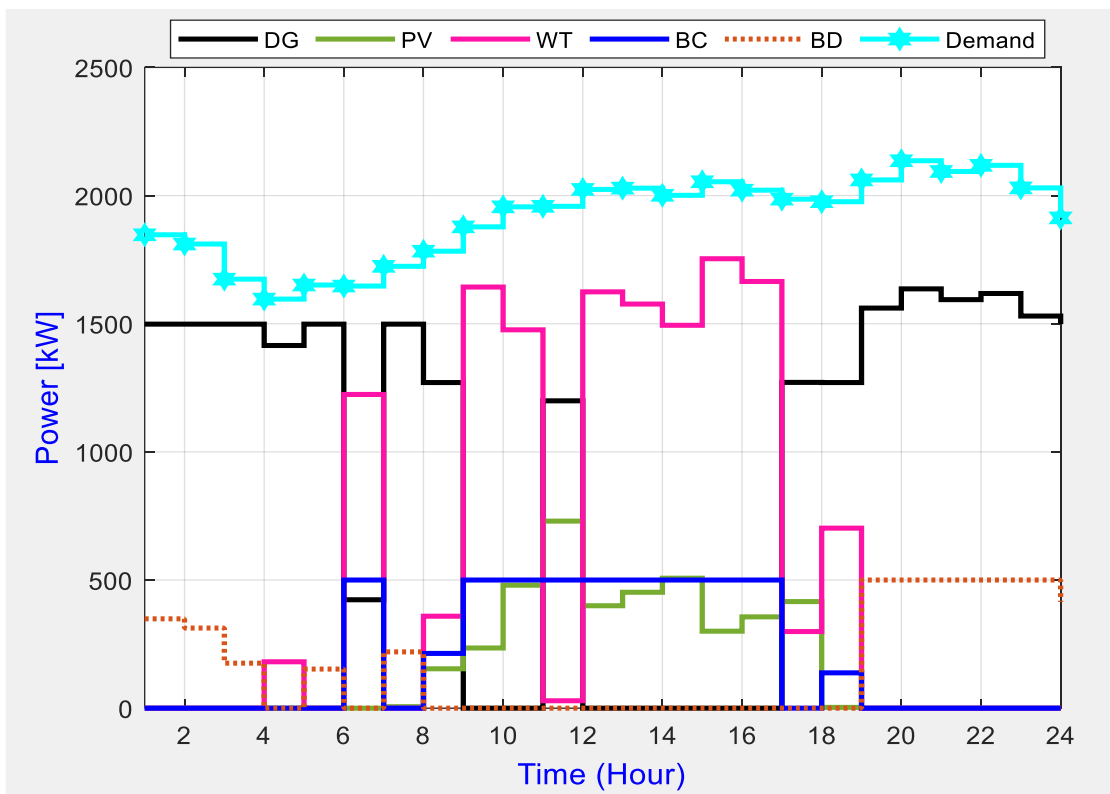Fig. 10 Summer Vacation day (17 April 2019) Power Flow

Fig. 11 Winter Study day (13 August 2019) Power Flow

The operation of the DG peaks at night when the WT and PV are unable to generate electricity, the power dissipation from the battery also ensures that there is net-zero active power deviation on the campus.
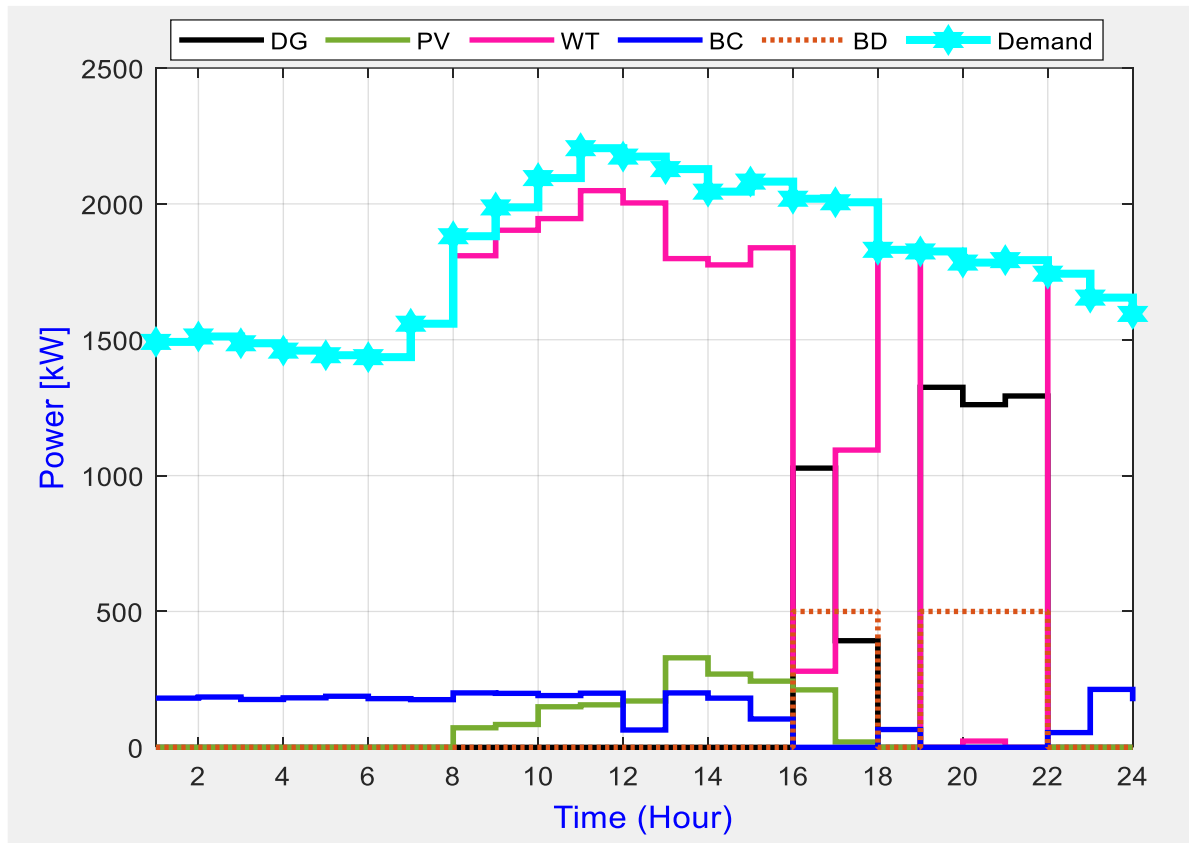
Fig. 12 Winter vacation day (25 June 2019) Power Flow

To investigate the fuel cost of the DG and fuel-saving cost during hybrid generation, Table 5 shows the financial implications of these two generation modes for the four scenarios analyzed on the Pietermaritzburg campus. It is clear that the hybrid generation saves fuel cost than running the DG full-time, however, the winter vacation day which experiences the highest penetration of WT has the least fuel cost when compared with other scenarios. The least savings period is the summer study day due to the low generation from the renewable energy sources. A comparative investigation of Tables 3 and Table 5 shows a contrasting result between the summer study period and the winter vacation period. While the summer study day is the highest fuel saving period at Howard campus, at the Pietermaritzburg campus, it is the least fuel-saving period. Similarly, the winter vacation day at the Pietermaritzburg campus shows the highest fuel saving period because of the availability of renewable energy sources on the Howard campus; it has the least fuel-saving owing to limited renewable energy available in the period.

Table 5 Fuel Cost Saving

	Summer ($/h)		Winter ($/h)	
	Study	Vacation	Study	Vacation
DG Only	50.31	41.50	45.97	43.24
Hybrid	38.90	12.56	23.78	5.30
Saving	**11.41**	**28.94**	**22.19**	**37.94**

The effects of location, climatic condition and academic sessions on the cost saving are reflected in Fig. 13 and Fig. 14. It can be observed the saving for both winter and summer are higher in PMB campus during the vacation period. This is as a result of low demand and higher wind speed in Pietermaritzburg. However, considering the study period (Fig. 14) in both campuses, Howard recorded a higher cost saving in summer while PMB has higher cost saving in winter. The Howard campus is located in the city of Durban that has a moderate temperature during summer, PMB campus is in the city of Pietermaritzburg (77 km north west of Durban) is hotter in summer and colder in winter. In a similar work [25], the cost saving was found to be lower in winter than the summer as a result of higher demand in winter as well as lower solar radiation in winter necessitating the use of conventional generators.
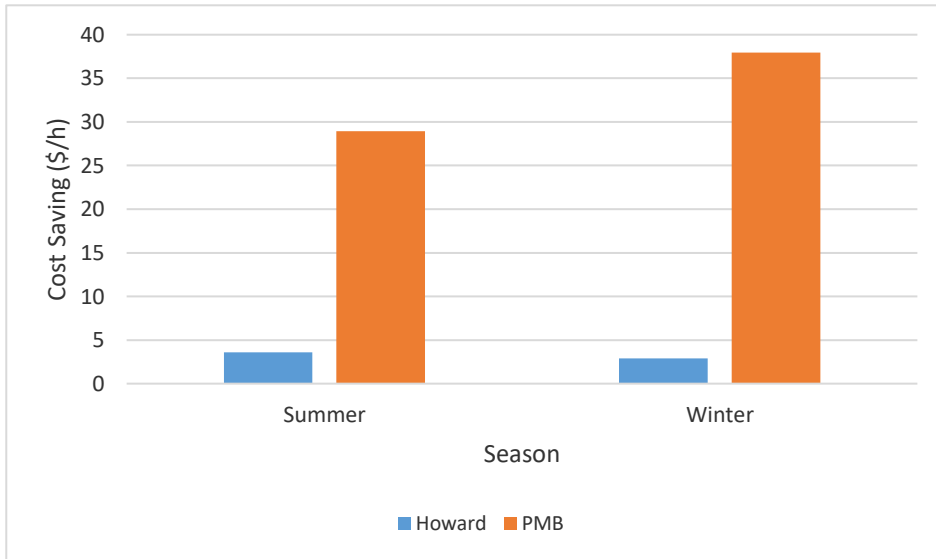

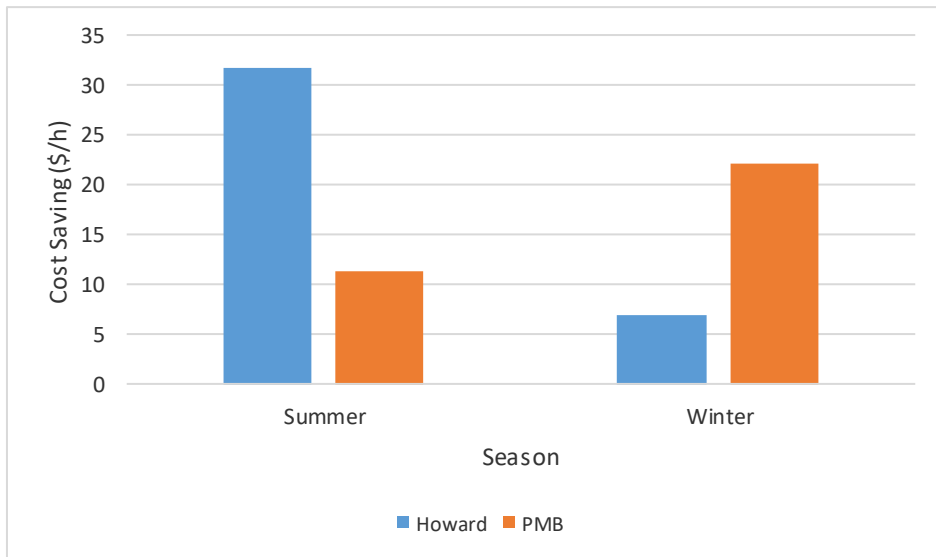Fig. 13 Cost saving comparison during vacation period

Fig. 14 Cost saving comparison during study period

Comparing the results on the two campuses shows no definite relationship between the various parameters considerd as a result of the variations in load, weather, academic displines on the two campuses.

Conclusions

The optimal power dispatch of a hybrid renewable energy system (HRES) has been presented and analyzed. The results reflect how changes in season, erratic nature of renewable energy source and academic activities affect the campus load, power generated by renewable energy source and hence the operational cost of the HRES. For instance, on the Howard campus, for both summer and winter vacation periods, the fuel costs for the HRES are close to the DG only resulting in little savings this is because the wind speeds are below the cut-off speed on those days. However, on the PMB campus, for both winter and summer seasons, fuel costs in the study periods are higher than that of vacation periods as a result of minimal academic activities on campus. In all, there are significant fuel cost savings in optimizing the HRES.

References

[1]   S. C. Madathil, Modeling and Analysis of Remote Off-grid Microgrids, PhD, Industrial Engineering, Clemson University, Clemson, South Carolina,USA, 2017.

[2]   Information on http://www .https://www.mtu-solutions.com/trmea/en/stories/technology/ electrification/successfully-disconnected.html.

[3]   M. Kaur, S. Dhundhara, Y.P. Verma, and S. Chauhan, Techno-economic analysis of photovoltaic-biomass-based microgrid system for reliable rural electrification, International Transactions on Electrical Energy Systems, 30 (2020) 1-20, doi: 10.1002/2050-7038.12347.

[4]   J. Ahmad, M. Imran, A. Khalid, et al., Techno economic analysis of a wind-photovoltaic-biomass hybrid renewable energy system for rural electrification: A case study of Kallar Kahar, Energy, 148 (2018) 208-234. doi: 10.1016/j.energy.2018.01.133.

[5]   G. Veilleux, T. Potisat, D. Pezim, et al.,Techno-economic analysis of microgrid projects for rural electrification: A systematic approach to the redesign of Koh Jik off-grid case study, Energy for Sustainable Development, 54 (2020) 1-13. doi: 10.1016/j.esd.2019.09.007.

[6]   M. R. Fuad, D. Octavianthy, and W. W. Purwanto, Techno-economic analysis of natural gas-fired microgrid for electricity, fresh water, and cold storage in rural area, AIP Conference Proceedings (2019) 20-28. doi: 10.1063/1.5095006

[7]   S. You, H. Tong, J. Armin-Hoiland, Y. W. Tong, and C.-H. Wang, Techno-economic and greenhouse gas savings assessment of decentralized biomass gasification for electrifying the rural areas of Indonesia, Applied Energy, 208 (2017) 495-510. doi: 10.1016/j.apenergy.2017.10.001.

[8]   S. Mazzola, M. Astolfi, and E. Macchi, The potential role of solid biomass for rural electrification: A techno economic analysis for a hybrid microgrid in India, Applied Energy, 169 (2016) 370-383. doi: 10.1016/j.apenergy.2016.02.051.

[9]   G. Oriti, A. L. Julian, N. Anglani, and G. D. Hernandez, Novel Economic Analysis to Design the Energy Storage Control System of a Remote Islanded Microgrid, IEEE Transactions on Industry Applications, 54 (2018) 6332-6342. doi: 10.1109/tia.2018.2853041.

[10]   K. E. Garcia, Optimization of microgrids at military remote base camps, MSc, NAVAL POSTGRADUATE SCHOOL, Monterey,California USA, 2017.

[11]   L. Olatomiwa, S. Mekhilef, A. S. N. Huda, and K. Sanusi, Techno-economic analysis of hybrid PV-diesel-battery and PV-wind-diesel-battery power systems for mobile BTS: the way forward for rural development, Energy Science & Engineering, 3 (2015) 271-285. doi: 10.1002/ese3.71.

[12]   J. S. Ojo, P. A. Owolawi, and A. M. Atoye, Designing a Green Power Delivery System for Base Transceiver Stations in Southwestern Nigeria, SAIEE Africa Research Journal, 110 (2019) 19-25. doi: 10.23919/SAIEE.2019.8643147.

[13]   S. T. Leholo, P. A. Owolawi, and K. T. Akindeji, Modelling and Optimization of Hybrid RE for Powering Remote GSM Base Station, in 2018 IEEE PES/IAS PowerAfrica, (2018) 869-874. doi: 10.1109/PowerAfrica.2018.8520994

[14]   N. Kalkan, K. Bercin, O. Cangul, M. G. Morales, M. M. K. M. Saleem, I. Marji, A. Metaxa, E. Tsigkogianni, A renewable energy solution for Highfield Campus of University of Southampton, Renewable and Sustainable Energy Reviews, 15 (2011) 2940-2959. doi: 10.1016/j.rser.2011.02.040.

[15]   V. B. Hau, M. Husein, I.-Y. Chung, D.-J. Won, W. Torre, and T. Nguyen, Analyzing the impact of renewable energy incentives and parameter uncertainties on financial feasibility of a campus microgrid, Energies, 11 (2018) 2446. doi: 10.3390/en11092446.

[16]   K. S. Saritha, S. Sreedharan, and U. Nair, A generalized setup of a campus microgrid - A case study, in International Conference on Energy, Communication, Data Analytics and Soft Computing (ICECDS), Chennai, India, (2017), 2182-2188. doi: 10.1109/ICECDS.2017.8389838

[17]   N. S. Savic, V. A. Katic, N. A. Katic, B. Dumnic, D. Milicevic, and Z. Corba, Techno-economic and environmental analysis of a microgrid concept in the university campus, in 2018 International Symposium on Industrial Electronics (INDEL), Banja Luka, Bosnia and Herzegovina, (2018). doi: 10.1109/INDEL.2018.8637613

[18]   L. Al-Ghussain, A. Darwish Ahmad, A. M. Abubaker, and M. A. Mohamed, An integrated photovoltaic/wind/biomass and hybrid energy storage systems towards 100% renewable energy microgrids in university campuses, Sustainable Energy Technologies and Assessments, 46 (2021) 101273. doi: 10.1016/j.seta.2021.101273.

[19]   J. J. D. Nesamalar, S. Suruthi, S. C. Raja, and K. Tamilarasu, Techno-economic analysis of both on-grid and off-grid hybrid energy system with sensitivity analysis for an educational institution, Energy Conversion and Management, 239 (2021) 114188. doi: 10.1016/j.enconman.2021.114188.

[20]   P. G. Arul, V. K. Ramachandaramutthy, and R. K. Rajkumar, Control strategies for a hybrid renewable energy system: A review, Renewable and Sustainable Energy Reviews, 42 (2015) 597-608. doi: http://dx.doi.org/10.1016/j.rser.2014.10.062.

[21]   C. Ammari, D. Belatrache, B. Touhami, and S. Makhloufi, Sizing, optimization, control and energy management of hybrid renewable energy system—A review, Energy and Built Environment, (2021). doi: 10.1016/j.enbenv.2021.04.002.

[22]   P. Gajewski and K. Pienkowski, Control of the Hybrid Renewable Energy System with Wind Turbine, Photovoltaic Panels and Battery Energy Storage, Energies, 14 (2021) 1595. doi: https://doi.org/10.3390/en14061595.

[23]   B. C. Phan and Y.-C. Lai, Control Strategy of a Hybrid Renewable Energy System Based on Reinforcement Learning Approach for an Isolated Microgrid, Appl. Sci., 9 (2019) 1-24. doi: http://doi:10.3390/app9194001.

[24]   M. H. Chung, Estimating Solar Insolation and Power Generation of Photovoltaic Systems Using Previous Day Weather Data, Advances in Civil Engineering, (2020) 1-13. doi: 10.1155/2020/8701368.

[25]   H. Tazvinga, X. Xia, and J. Zhang, Minimum cost solution of photovoltaic–diesel–battery hybrid power systems for remote consumers, Solar Energy, 96 (2013) 292-299. doi: 10.1016/j.solener.2013.07.030.

[26]   H. Tazvinga, Energy optimisation and management of off-grid hybrid power supply systems, Doctor of Philosophy, Department of Electrical, Electronic and computer engineering, University of Pretoria, Pretoria, 2015.

[27]   L. Arturo Soriano, W. Yu, and J. d. J. Rubio, Modeling and Control of Wind Turbine, Mathematical Problems in Engineering, (2013) 1-13. doi: 10.1155/2013/982597.

[28]   S. Lalljith, A. G. Swanson, and A. Goudarzi, An intelligent alternating current-optimal power flow for reduction of pollutant gases with incorporation of variable generation resources, Journal of Energy in Southern Africa, 31 (2020) 40-61. doi: 10.17159/2413-3051/2020/v31i1a7008.

[29]   M. H. H. Albadi, On Techno-Economic Evaluation of Wind-Based DG, Doctor of Philosophy, Electrical and Computer Engineering, University of Waterloo, Waterloo, Ontario, Canada, 2010.